

Electronic Supplementary Information for

Hydrothermal synthesis of palladium nitrides as robust multifunctional electrocatalysts for fuel cells

Ruiyun Guo, Ke Zhang, Yaming Liu, Yucheng He, Chao Wu* and Mingshang Jin*

^aFrontier Institute of Science and Technology and State Key Laboratory of Multiphase Flow in Power Engineering, Xi'an Jiaotong University, Xi'an, Shaanxi 710049, China.

^bFrontier Institute of Science and Technology, Xi'an Jiaotong University, Xi'an, Shaanxi 710049, China.

*To whom correspondence should be addressed. E-mail: jinm@mail.xjtu.edu.cn.

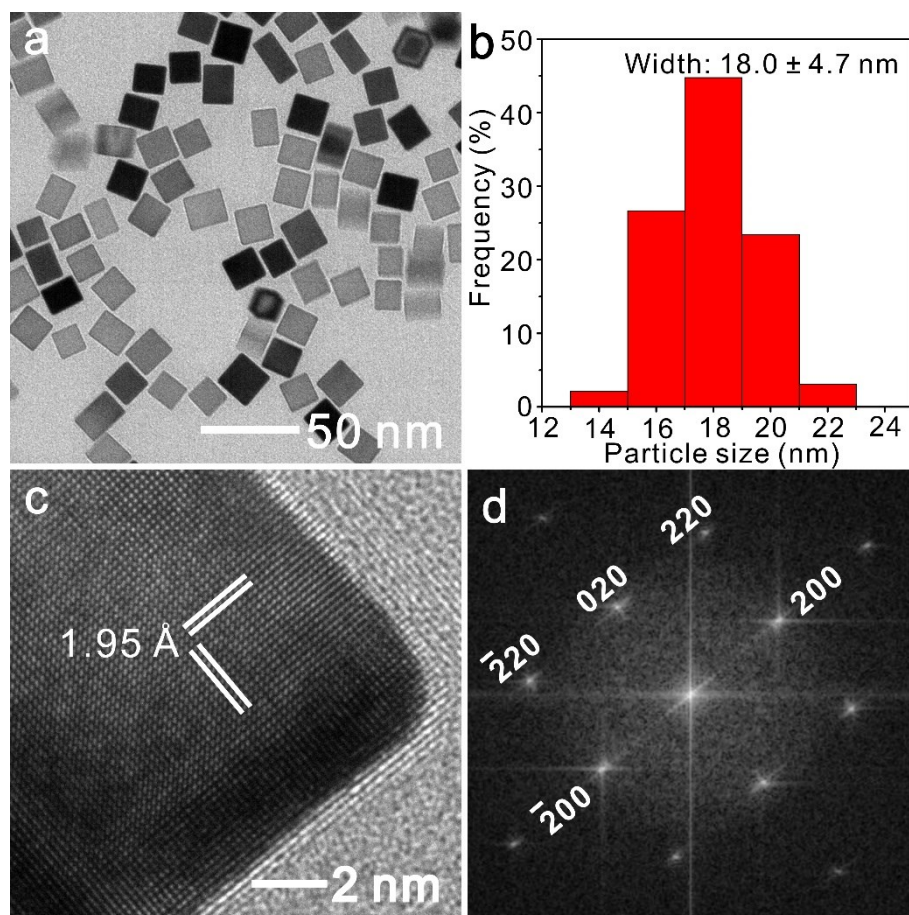


Figure S1. (a) TEM image of the obtained Pd nanocubes and (b) corresponding histogram of size distribution. (c) HRTEM image of an individual Pd nanocube and (d) FFT pattern of Pd nanocube shown in (c) recorded along the $\langle 001 \rangle$ zone axis.

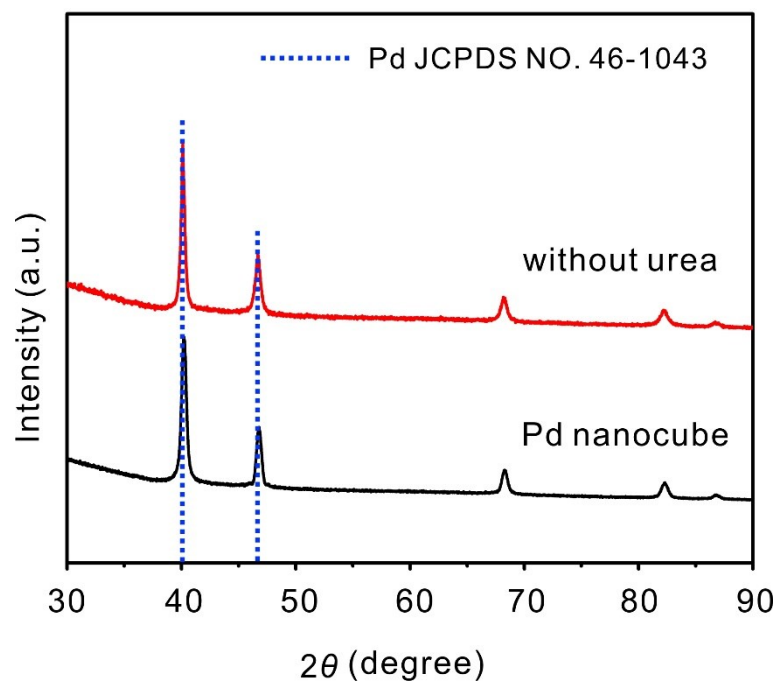


Figure S2. XRD patterns of Pd nanocubes and the products obtained using the standard procedures, except for the addition of urea.

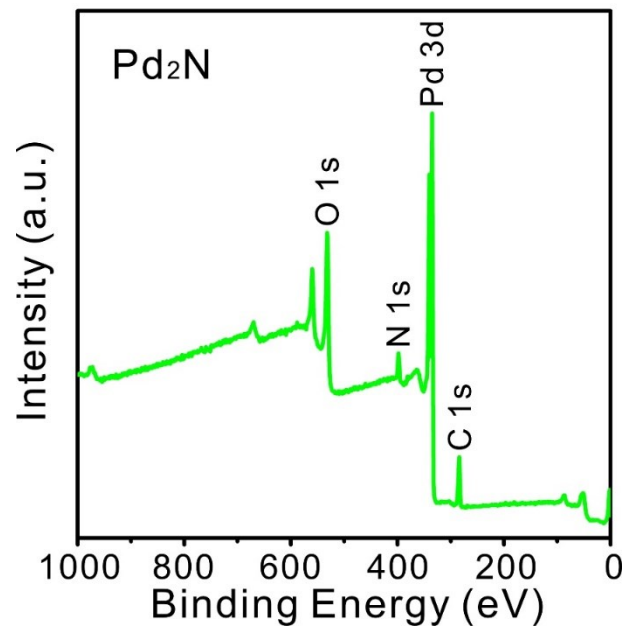


Figure S3. XPS spectrum of Pd₂N nanocrystals.

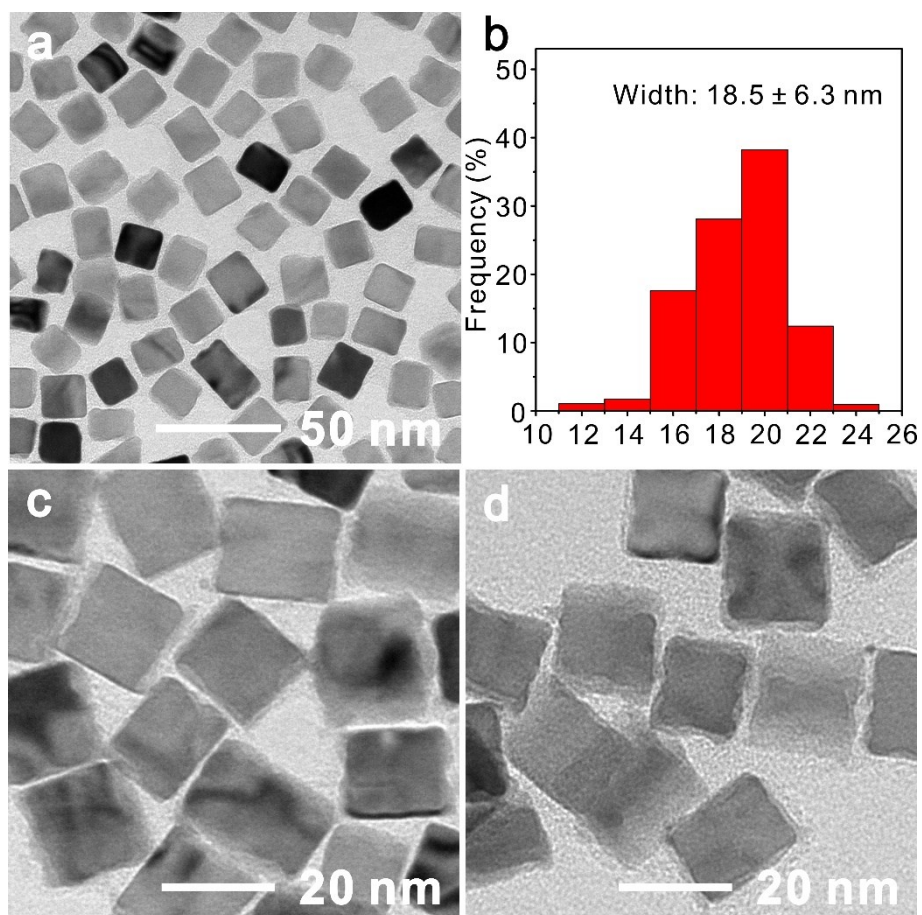


Figure S4. (a) Low and (c, d) high magnification TEM images of Pd₂N nanocrystals, and (b) the corresponding histogram of size distribution counted from (a).

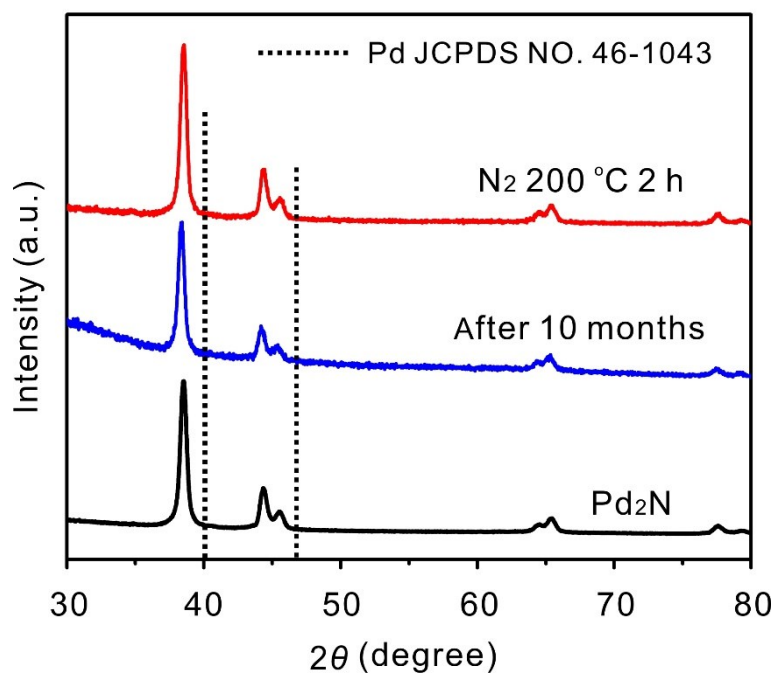


Figure S5. XRD patterns of Pd₂N nanocrystals after 10 months of storage in air and annealing under N₂ atmosphere at 200 °C for 2 h, respectively.

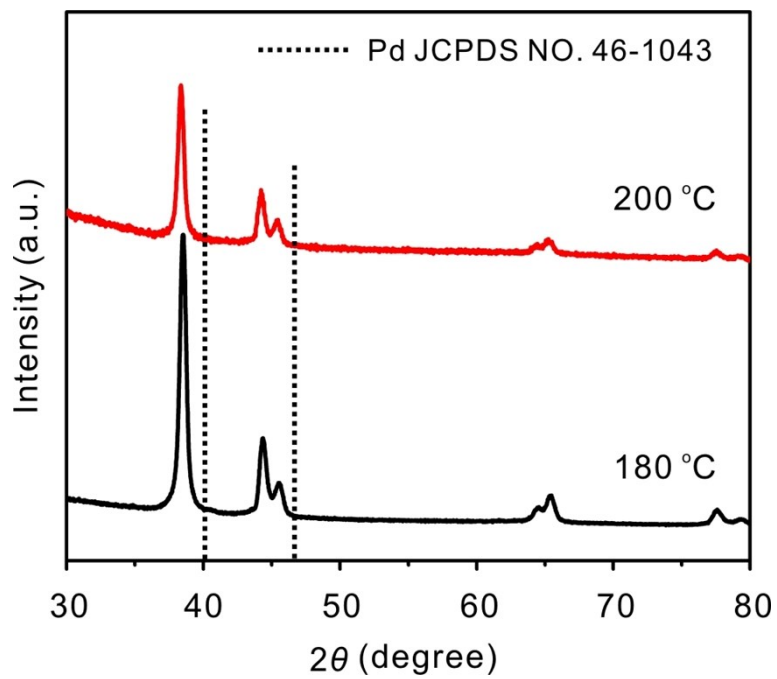


Figure S6. XRD patterns of the products obtained with the reaction temperature increased from 180 to 200 °C under the standard synthetic conditions.

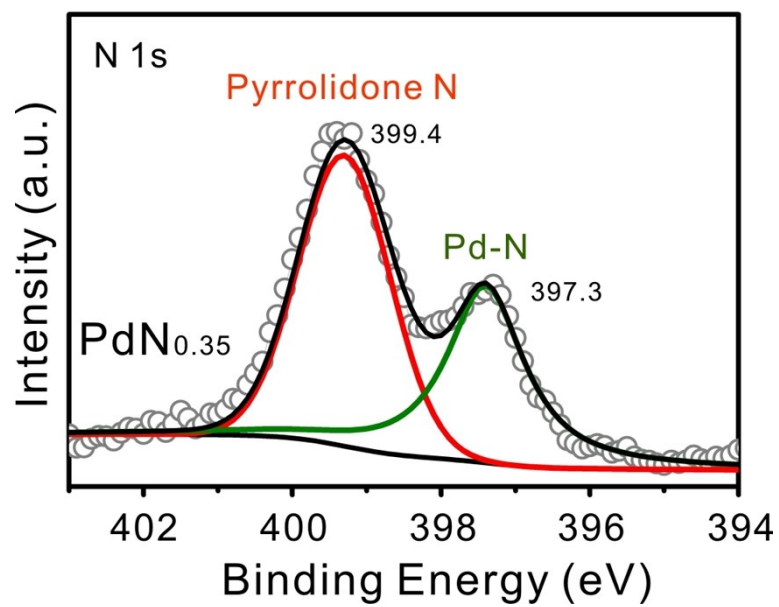


Figure S7. XPS analysis of N 1s in PdN_{0.35} nanocrystals.

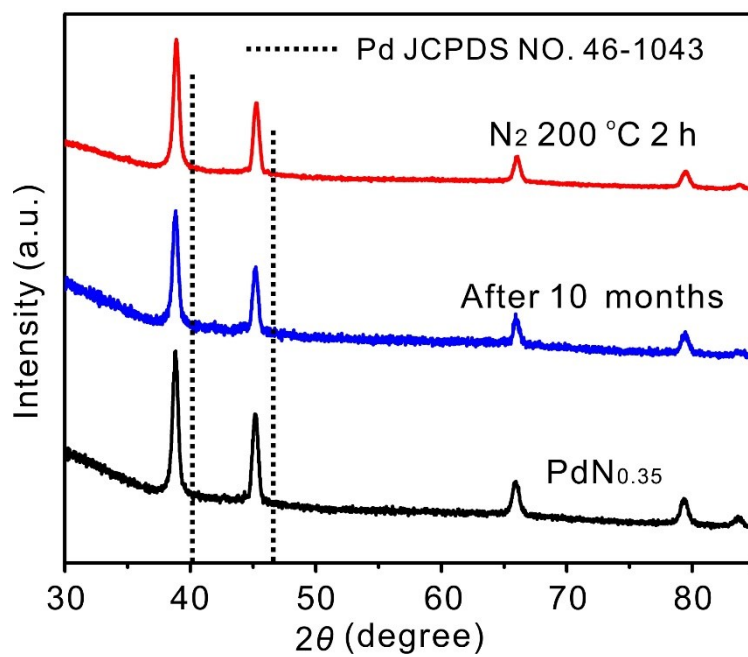


Figure S8. XRD patterns of PdN_{0.35} nanocrystals after 10 months of storage in air and annealing under N₂ atmosphere at 200 °C for 2 h, respectively.

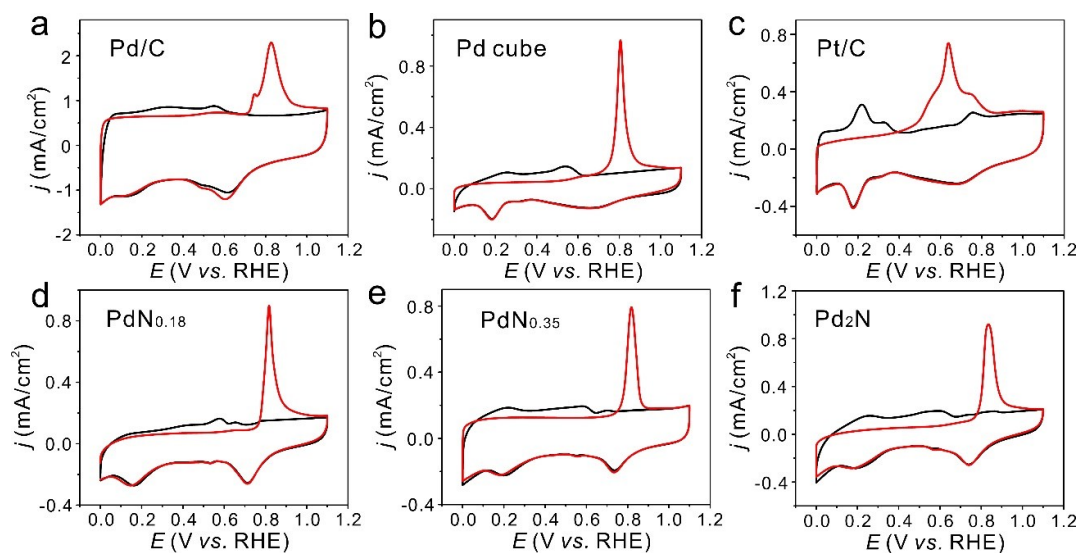


Figure S9. CO stripping voltammograms of different catalysts: (a) commercial Pd/C, (b) Pd nanocubes, (c) commercial Pt/C, (d) PdN_{0.18}, (e) PdN_{0.35} and (f) Pd₂N nanocrystals, respectively. The red line is the first scan and the black line is the second scan.

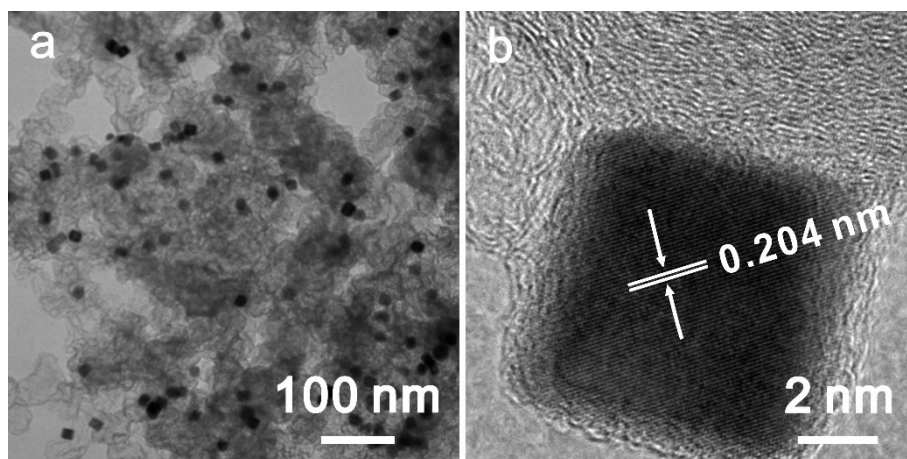


Figure S10. (a) Low magnification TEM and (b) HRTEM images of Pd₂N nanocrystals after 10,000-cycles ADTs.

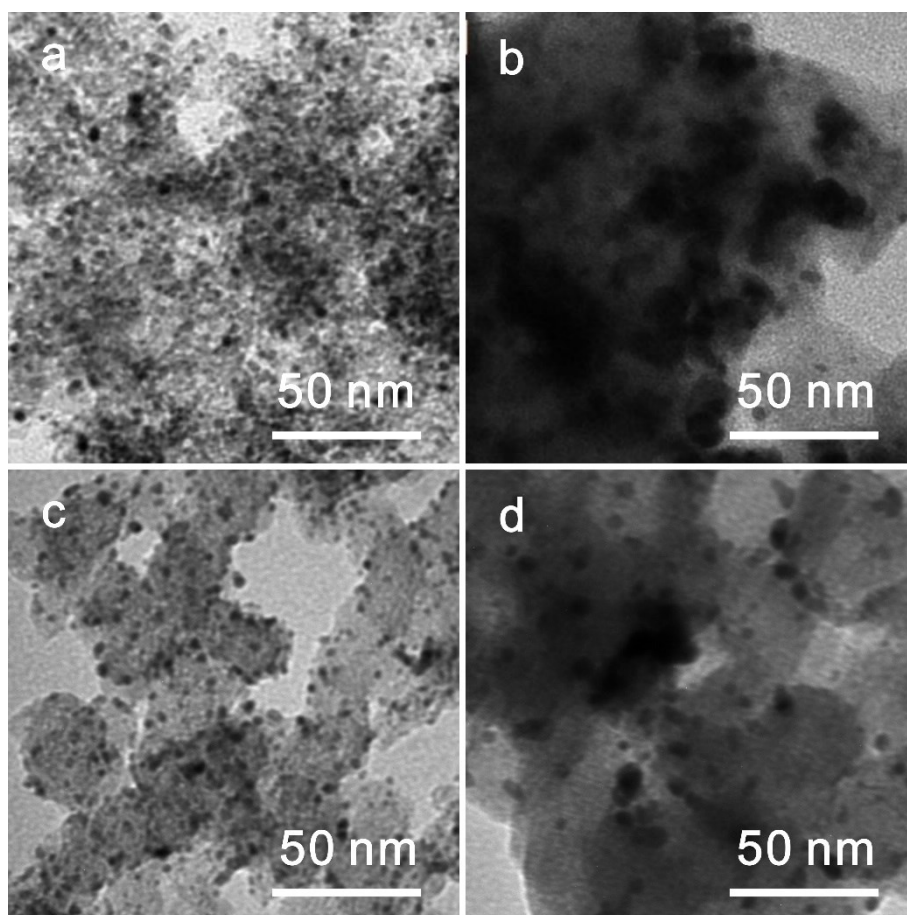


Figure S11. Representative TEM images of commercial Pd/C and Pt/C catalyst (a, c) before and (b, d) after 10,000-cycles ADTs.

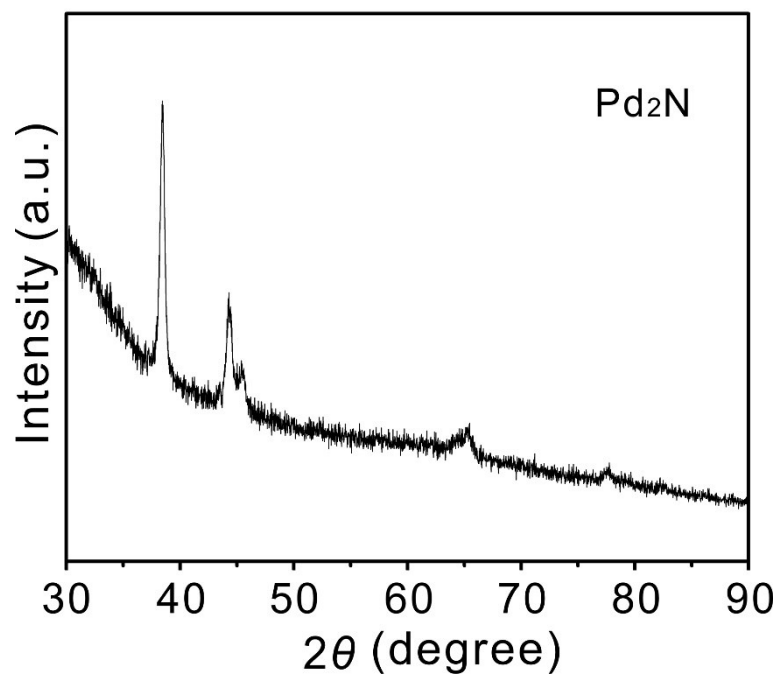


Figure S12. XRD pattern of Pd₂N nanocrystals after 10,000-cycles ADTs.

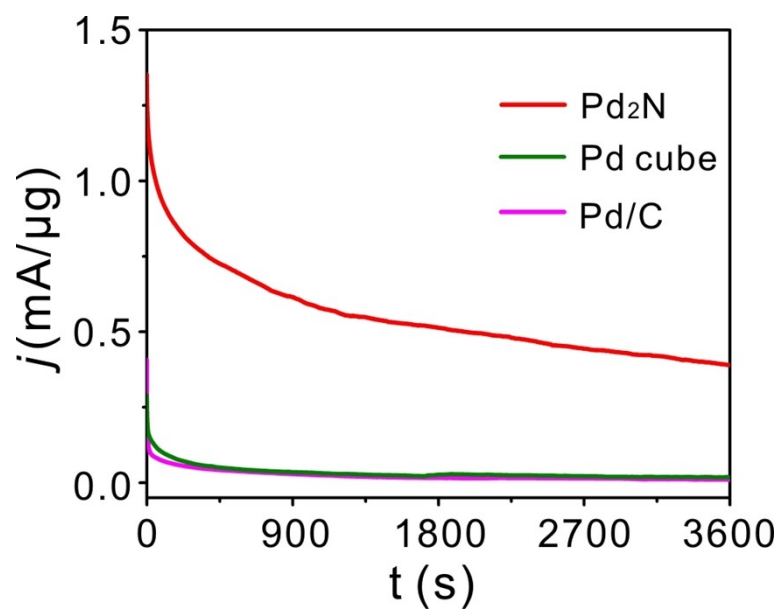


Figure S13. Comparison of FAOR chronoamperometric stability profiles of Pd₂N nanocrystals, the original Pd nanocubes, and commercial Pd/C catalysts at the potential of 0.4 V_{RHE}.

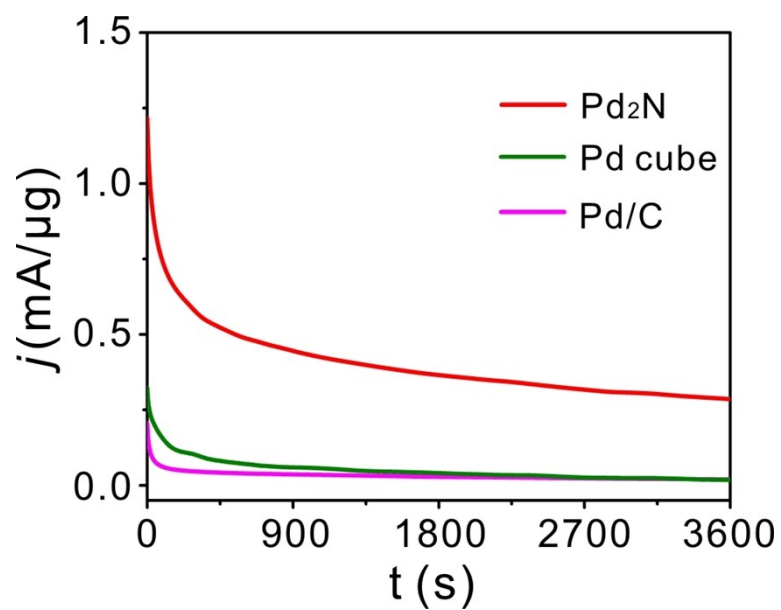


Figure S14. Comparison of MOR chronoamperometric stability profiles of Pd₂N nanocrystals, the original Pd nanocubes, and commercial Pd/C catalyst at the potential of 0.75 V_{RHE}.

Table S1. Calculated XRD parameters of tetragonal Pd₂N nanocrystals.

2 Theta (°)	d-spacing (Å)	Intensity (a. u.)	(hkl)
38.523	2.3351	3640740.73	112
44.427	2.0375	1575247.36	020
45.480	1.9928	705944.29	004
64.642	1.4407	487656.15	220
65.462	1.4246	902328.32	024
77.840	1.2261	925727.00	312
79.358	1.2064	404563.56	116
82.563	1.1675	472153.63	224

Table S2. XRD and XPS parameters for the original Pd nanocubes and the obtained PdN_x nanocrystals.

Samples	Urea amount (mg)	{111} peak position in $2\theta(^{\circ})$	Binding energy of $3d_{3/2}$ (eV)	Binding energy of $3d_{5/2}$ (eV)
Pd cube	0	40.11	340.4	335.1
PdN _{0.08}	75	39.81	340.5	335.2
PdN _{0.18}	100	39.40	340.6	335.3
PdN _{0.26}	150	39.11	340.8	335.5
PdN _{0.35}	200	38.82	340.9	335.6

Table S3. Specific ECSAs, $E_{1/2}$ values, and the specific and mass activities of the catalysts for ORR in 0.1 M KOH.

Samples	Specific ECSA ($\text{m}^2 \text{g}^{-1}$)	$E_{1/2}$ value (V)	Specific activity (@0.9 V mA cm^{-2})	Mass activity (@0.9 V A mg^{-1})
Commercial Pd/C	42.3	0.821	0.13	0.055
Pd cube	22.9	0.843	0.35	0.08
Commercial Pt/C	61.1	0.862	0.18	0.11
PdN _{0.18}	29.5	0.893	1.49	0.44
PdN _{0.35}	32.8	0.901	1.80	0.59
Pd ₂ N	39.9	0.916	2.08	0.83

Table S4. A list of ORR performance of the most advanced Pd-based electrocatalysts from recently published works in alkaline electrolyte.

Entry	Catalysts	Electrolyte solution	Mass activity (@0.9 V A mg ⁻¹)	Specific activity (@0.9 V mA cm ⁻²)	References
1	Pd ₂ N/C	0.1 M KOH	0.83	2.08	This work
2	PdN _{0.35} /C	0.1 M KOH	0.59	1.80	This work
3	Pd-Te hexagonal nanoplates/C	0.1 M KOH	0.30	N/A	<i>Sci. Adv.</i> , 2020, 6 , eaba9731
4	Pd ₃ Pb/Pd nanosheets/C	0.1 M KOH	0.574	1.31	<i>Nano Lett.</i> , 2019, 19 , 1336-1342.
5	Pd ₅₉ Cu ₃₀ Co ₁₁	0.1 M KOH	0.38	0.90	<i>Nat Commun.</i> , 2018, 9 , 3702.
6	Au nanowire @Pd _{0.1} @PEI	0.1 M KOH	0.295	N/A	<i>ACS Catal.</i> , 2018, 8 , 11287-11295.
7	Pd ₃ Pb nanoplates	0.1 M KOH	0.78	N/A	<i>Small Methods</i> , 2018, 2 , 1700331.
8	Pd ₆ Ni icosahedra	1 M KOH	0.22	0.66	<i>Sci. Adv.</i> , 2018, 4 , 8817.
9	Pd ₃ Pb tripods/C	0.1 M KOH	0.56	1.76	<i>Chem</i> , 2018, 4 , 359-371.
10	PdCu tetrapod	0.1 M KOH	0.29	0.73	<i>ChemCatChem</i> , 2018, 10 , 925-930.
11	Pd ₃ Pb nanowire networks	0.1 M KOH	0.61	15.7	<i>J. Mater. Chem. A</i> , 2017, 5 , 23952-23959.
12	Ni@Pd ₃ /C	0.1 M KOH	0.038	0.13	<i>J. Mater. Chem. A</i> , 2017, 5 , 9233-9240.
13	Pd@PtNi	0.1 M KOH	0.0733	N/A	<i>J. Power Sources</i> , 2017, 365 , 26-33.
14	Pd-B/C	0.1 M KOH	0.602	0.17	<i>J. Phy. Chem. C</i> , 2017, 121 , 3416-3423.
15	O-Pd ₆ Sn ₃ Co/C	0.5 M KOH	0.1348@0.85 V	0.5653@0.85 V	<i>J. Electroanal. Chem.</i> , 2017, 789 , 167-173.
16	ordered Pd ₃ Pb/C	0.1 M KOH	0.1689	N/A	<i>Nano Lett.</i> , 2016, 16 , 2560-2566.
17	Pd@Pt core-island shell	0.1 M KOH	0.26	1.224	<i>Nanoscale</i> , 2016, 8 , 1698-1703.
18	PdCuCo NPs/C-375°C	0.1 M NaOH	0.13	N/A	<i>Angew. Chem. Int. Ed.</i> , 2016, 55 , 9030-9035.
19	PdMn/C-BAE	0.1 M KOH	0.093@0.85 V	0.35@0.85 V	<i>J. Mater. Chem. A</i> , 2016, 4 , 8337-8349.
20	Pd-Ni/CNFN 1:2	0.1 M KOH	0.098@0.85 V	N/A	<i>Int. J. Hydrogen Energy</i> , 2016, 41 , 22538-22546.
21	ordered Pd ₃ Fe/C	0.1 M KOH	0.0974	N/A	<i>J. Am. Chem. Soc.</i> , 2015, 137 , 7278-7281.
22	AuPd alloyed flowerlike	0.1 M KOH	0.215@0.71 V	0.55@0.71 V	<i>J. Mater. Chem. A</i> , 2015, 3 , 5352-5359.

23	Au/Cu ₄₀ Pd ₆₀ NPs	0.1 M KOH	0.43@-0.1V vs. Ag/AgCl	N/A	<i>J. Am. Chem. Soc.</i> , 2014, 136 , 15026-15033.
24	Pd-P (3)	0.1 M KOH	1.79 @ 0.85 V	2.31@0.85 V	<i>J. Am. Chem. Soc.</i> , 2014, 136 , 5217-5220.
25	Pd/W ₁₈ O ₄₉ hybrids	0.1 M KOH	0.216	0.45	<i>J. Am. Chem. Soc.</i> , 2014, 136 , 11687-11697.
26	Pd nanoparticles	0.1 M KOH	0.038	0.10	<i>Nat. Commun.</i> , 2014, 5 , 5185.
27	AuPdCo/C intermetallic	0.1 M KOH	0.13	N/A	<i>ACS Catal.</i> , 2020, 10 , 9967-9976.
28	Pt ₃₇ Cu ₅₆ Au ₇	0.1 M KOH	0.871	1.85	<i>Chem. Commun.</i> , 2018, 54 , 7058-7061.
29	Pd ₄ Fe nanoflowers/C	0.1 M KOH	0.975	2.78	<i>Nanoscale</i> , 2019, 11 , 17301-17307.
30	Pd ₃ Pb nanoflowers/C	0.1 M KOH	1.14	4.7	<i>Nature</i> , 2019, 574 , 81-85.
31	PdMo bimetallic/C	0.1 M KOH	16.37	11.64	

N/A: not available